

Gas-Phase Synthesis of 3-Vinylcyclopropene via the Crossed Beam Reaction of the Methylidyne Radical (CH ; $\text{X}^2\Pi$) with 1,3-Butadiene ($\text{CH}_2\text{CHCHCH}_2$; X^1A_g)

Chao He,^[a] Long Zhao,^[a] Srinivas Doddipatla,^[a] Aaron M. Thomas,^[a] Anatoliy A. Nikolayev,^[b] Galiya R. Galimova,^[b, c] Valeriy N. Azyazov,^[b, d] Alexander M. Mebel,^{*[c]} and Ralf I. Kaiser^{*[a]}

The crossed molecular beam reactions of the methylidyne radical (CH ; $\text{X}^2\Pi$) with 1,3-butadiene ($\text{CH}_2\text{CHCHCH}_2$; X^1A_g) along with their (partially) deuterated counterparts were performed at collision energies of 20.8 kJ mol^{-1} under single collision conditions. Combining our laboratory data with *ab initio* calculations, we reveal that the methylidyne radical may add barrierlessly to the terminal carbon atom and/or carbon–carbon double bond of 1,3-butadiene, leading to doublet C_5H_7 intermediates with life times longer than the rotation periods.

These collision complexes undergo non-statistical unimolecular decomposition through hydrogen atom emission yielding the cyclic cis- and trans-3-vinyl-cyclopropene products with reaction exoergicities of $119 \pm 42 \text{ kJ mol}^{-1}$. Since this reaction is barrierless, exoergic, and all transition states are located below the energy of the separated reactants, these cyclic C_5H_6 products are predicted to be accessed even in low-temperature environments, such as in hydrocarbon-rich atmospheres of planets and cold molecular clouds such as TMC-1.

1. Introduction

During the last decades, the exploration of the formation mechanisms of C_5 hydrocarbon species has drawn considerable attention from the physical, theoretical, and combustion chemistry and astrochemistry communities due to the importance of C_5 hydrocarbons as potential precursors to polycyclic aromatic hydrocarbons (PAHs) in combustion processes and in extraterrestrial environments such as in circumstellar envelopes of dying carbon stars (IRC + 10216) and in cold molecular clouds (TMC-1, OMC-1).^[1–21] High concentrations of C_5 species were observed in fuel-rich flames.^[1–3] Hansen and co-workers conducted a systematic study on the identification of C_5 species in hydrocarbon-rich flames fueled by allene (H_2CCCH_2), propyne (CH_3CCH), cyclopentene ($\text{c-C}_5\text{H}_8$), and benzene (C_6H_6).^[1,2] Combined with kinetic models, C_5H_x ($x = 2–6$, and 8) molecules have been detected exploiting molecular-beam mass spectrometry sampling via tunable vacuum ultraviolet (VUV) synchrotron photoionization.^[1] The C_5 species identified consisted of (1) C_5H_2 (1,2-cyclopentadien-4-yne, c-CCHCCCH), (2) C_5H_3 (2,4-pentadiynyl-1 radical, H_2CCCCCH ; 1,4-pentadiynyl-3 radical, HCCCHCCCH ; cyclopenta-1,2,3-triene radical, c-CCHCHCCCH), (3) C_5H_4 (1,2,3-4-

pentatetraene, $\text{CH}_2\text{CCCCH}_2$; penta-1,2-dien-4-yne, $\text{CH}_2\text{CCHCCCH}$; 1,3-pentadiyne, CHCCCCCH_3 ; 1,4-pentadiyne, CHCCH_2CCH), (4) C_5H_5 (cyclopentadienyl radical, $\text{c-C}_5\text{H}_5$), (5) C_5H_6 (1,3-cyclopentadiene, $\text{c-C}_5\text{H}_6$; 1-penten-3-yne, $\text{CH}_2\text{CHCCCCCH}_3$; 3-penten-1-yne $\text{CH}_3\text{CHCHCCCH}$; pent-1-en-4-yne, $\text{CH}_2\text{CHCH}_2\text{CCH}$), and (6) C_5H_8 (1,3-pentadiene, $\text{CH}_2(\text{CH})_3\text{CH}_3$; cyclopentene, $(\text{CH}_2)_3(\text{CH})_2$; 2-pentyne, $\text{CH}_3\text{CCCH}_2\text{CH}_3$; 1,4-pentadiene, $\text{CH}_2\text{CHCH}_2\text{CHCH}_2$). Further, two C_5H_3 isomers, the 2,4-pentadiynyl-1 ($i\text{-C}_5\text{H}_3$, H_2CCCCCH) and 1,4-pentadiynyl-3 ($n\text{-C}_5\text{H}_3$, HCCCHCCCH) along with two C_5H_5 isomers (1-vinylpropargyl, $\text{CH}_2\text{CHCHCCCH}$; cyclopentadienyl, $\text{c-C}_5\text{H}_5$) were identified in benzene/oxygen flames.^[3] In deep space, the highly reactive pentynylidene radical (C_5H) has been first discovered in the envelope of the carbon star IRC + 10216 via the observation of six rotational transitions^[4–6] and also in the laboratory via crossed molecular beams of ground state carbon atoms ($\text{C}(^3\text{P})$) and diacetylene (C_4H_2).^[22] Three years later, the C_5 molecule was detected in IRC + 10216 as well.^[7]

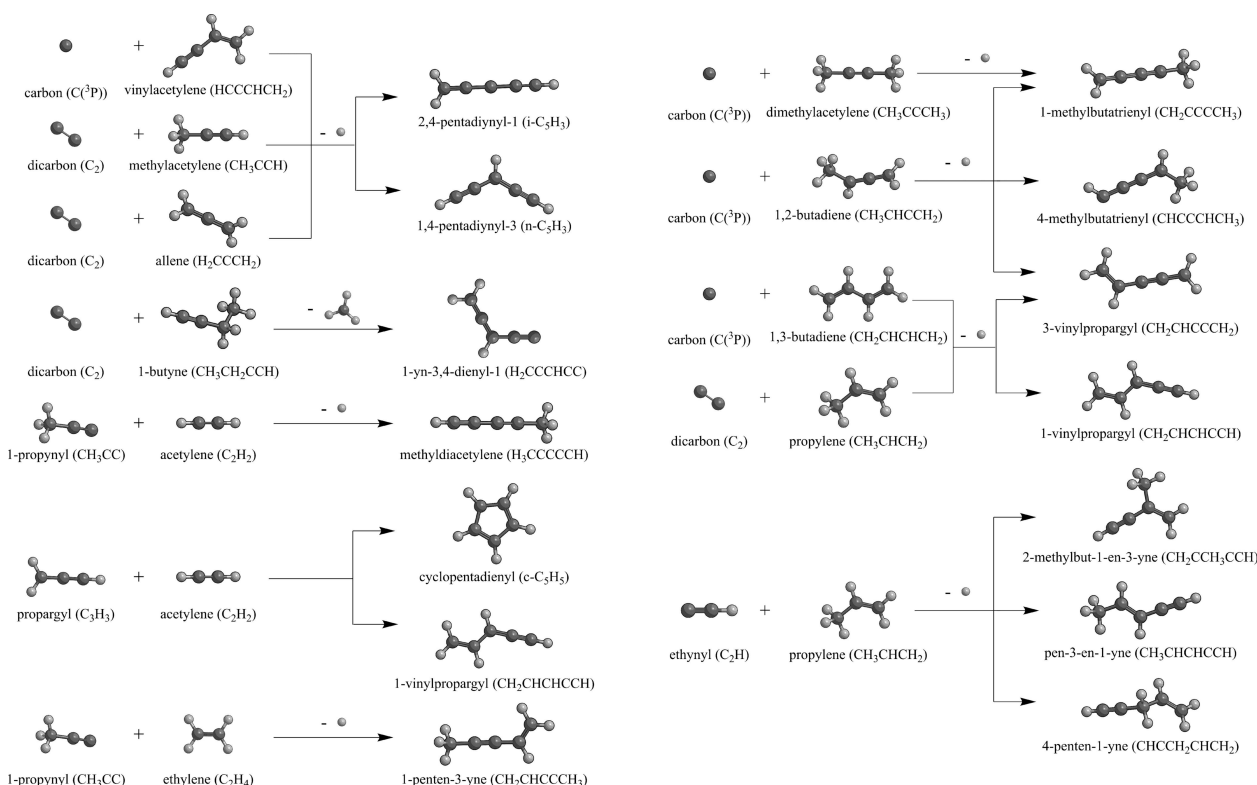
Experimental studies along with theoretical calculations provide compelling evidence that critical C_5H_x isomers ($x = 3–7$) can be formed via bimolecular reactions involving neutral-neutral reactions.^[8–21] Crossed molecular beams reactions of the ground state carbon atoms ($\text{C}(^3\text{P})$) with vinylacetylene (HCCCHCH_2) revealed the formation of distinct C_5H_3 isomers.^[15] The carbon atom was found to attack the double and/or triple bond of vinylacetylene without entrance barrier forming long-lived C_5H_4 complex(es) eventually decomposing via atomic hydrogen loss to the 2,4-pentadiynyl-1 radical ($i\text{-C}_5\text{H}_3$, H_2CCCCCH) and the 1,4-pentadiynyl-3 radical ($n\text{-C}_5\text{H}_3$, HCCCHCCCH).^[15] Both radicals $i\text{-C}_5\text{H}_3$ and $n\text{-C}_5\text{H}_3$ are also defined as the products in the bimolecular reactions of dicarbon ($\text{C}_2(\text{X}^1\Sigma_g^+/\text{a}^3\Pi_u)$) with methylacetylene (CH_3CCH) and allene (CH_2CCH_2).^[11–14,19] Combining experimental data with *ab initio* electronic structure and statistical Rice-Ramsperger-Kassel-Marcus (RRKM) calculations allowed us to show that the resonantly

[a] C. He, L. Zhao, S. Doddipatla, A. M. Thomas, Prof. R. I. Kaiser
Department of Chemistry, University of Hawai'i at Manoa, Honolulu, Hawaii 96822, USA
E-mail: ralfk@hawaii.edu
[b] A. A. Nikolayev, G. R. Galimova, V. N. Azyazov
Samara National Research University, Samara 443086, Russian Federation
[c] G. R. Galimova, Prof. A. M. Mebel
Department of Chemistry and Biochemistry, Florida International University, Miami, Florida 33199, USA
E-mail: mebel@fiu.edu
[d] V. N. Azyazov
Lebedev Physical Institute, Samara 443011, Russian Federation
Supporting information for this article is available on the WWW under
<https://doi.org/10.1002/cphc.202000183>

stabilized penta-1-yn-3,4-dienyl-1 (C_5H_3 ; $H_2CCCHCC$) radical along with the methyl radical (CH_3) are exclusively formed on the triplet surface in the dicarbon (C_2 ($X^1\Sigma_g^+/\alpha^3\Pi_u$))-1-butyne (CH_3CH_2CCH) system.^[19] Further, the formation mechanism of multiple C_5H_4 isomers was studied via the crossed molecular beams reaction of the 1-propynyl (CH_3CC) radical with acetylene ($HCCH$) under single-collision conditions.^[20] By analyzing experimental scattering data and merging these results with electronic structure calculations, methyldiacetylene (CH_3CCCCH) was revealed to be exclusively formed with hydrogen emission from the acetylene reactant.^[20] da Silva explored the C_5H_5 PES using the composite G3X-K model chemistry. The study revealed that both the cyclopentadienyl ($c-C_5H_5$) and 1-vinylpropargyl ($l-C_5H_5$; $CH_2CHCHCCH$) radicals were formed in the reaction of acetylene (C_2H_2) with the propargyl radical (C_3H_3) through an entrance barrier of 55 kJ mol⁻¹.^[18] Besides, acyclic C_5H_5 radicals were generated via barrierless reactions between carbon atoms ($C(^3P)$) with three C_4H_6 isomers [1,3-butadiene ($CH_2CHCHCH_2$),^[8] 1,2-butadiene (CH_2CCHCH_3),^[10] dimethylacetylene (CH_3CCCCH_3)^[9]] and in the reaction of singlet/triplet dicarbon (C_2) with propylene (CH_2CHCH_3).^[16] In addition, quantum chemical calculations combined with canonical transition state theory and Rice-Ramsperger-Kassel-Marcus/Master Equation (RRKM/ME) theory revealed the mechanism of the reaction of the ethynyl radical (C_2H) with propylene (CH_3CHCH_2) involving the formation of 2-methylbut-1-en-3-yne (C_5H_6 ; CH_2CCH_3CCH), pent-3-en-1-yne (C_5H_6 ; $CHCCHCHCH_3$) and 4-penten-1-yne (C_5H_6 ; $CHCCH_2CHCH_2$) via hydrogen emission.^[17] Crossed beams studies of the propynyl–ethylene system

exposed chemical dynamics, which are initiated by the barrierless addition of the 1-propynyl radical to the π -electron density of ethylene leading to a long-lived doublet C_5H_7 intermediate(s). The final product was 1-penten-3-yne (C_5H_6 ; $CH_2CHCCCCH_3$) with the hydrogen atom ejected solely from ethylene reactant (Scheme 1).^[21]

The aforementioned pathways exposed that the underlying formation mechanisms of C_5 hydrocarbon species are very complex and still poorly understood. To further shed light on the chemistry and chemical dynamics of C_5 hydrocarbon species, we present here the results of a study of the bimolecular reaction of the methylidyne radical (CH ; $X^2\Pi$) with 1,3-butadiene (C_4H_6 ; X^1A_g) along with their partially deuterated reactants at collision energies of 20.8 kJ mol⁻¹ under single-collision conditions. By combining these experimental data with electronic structure calculations of the C_5H_7 potential energy surface (PES), we demonstrate that cis- and trans-3-vinyl-cyclopropene are formed via addition of the methylidyne radical to the terminal carbon atom and/or carbon–carbon double bond of the 1,3-butadiene reactant. The disagreements between statistical computations and experiments are discussed, and reaction mechanism(s) are proposed.



Scheme 1. Bimolecular reactions leading to distinct C_5H_x isomers ($x=3-6$).

2. Methods

2.1. Experimental

The bimolecular reactions of the methylidyne ($\text{CH}; \text{X}^2\Pi$) radical with 1,3-butadiene ($\text{CH}_2\text{CHCHCH}_2; \text{X}^1\text{A}_g$) and the partially deuterated reactants were studied under single collision conditions in a crossed molecular beams machine at the University of Hawaii.^[23] In the primary chamber, a pulsed supersonic methylidyne beam was generated via photodissociation (COMPex 110, Coherent, Inc; 248 nm; 30 Hz) of a gas mixture of bromoform (CHBr_3 , Aldrich Chemistry, $\geq 99\%$) seeded in helium (99.9999%; AirGas) held in a stainless steel bubbler at 283 K with a stagnation pressure of 2.2 atm.^[24,25] The molecular beam was skimmed and velocity selected by a four-slot chopper wheel yielding a peak velocity of $v_p = 1836 \pm 15 \text{ m s}^{-1}$ and speed ratio S of 11.6 ± 0.9 of the methylidyne beam (Table 1). Typical rotational temperatures of the methylidyne radical were determined to be $14 \pm 1 \text{ K}$ exploiting laser induced fluorescence (LIF).^[26] A supersonic beam of neat 1,3-butadiene (Aldrich Chemistry, 99%+) at a backing pressure of 550 Torr with $v_p = 777 \pm 12 \text{ m s}^{-1}$ and $S = 9.5 \pm 0.3$ was produced in the secondary chamber; this beam crossed perpendicularly with the section of the methylidyne beam resulting in a collision energy E_c of $20.8 \pm 0.4 \text{ kJ mol}^{-1}$ and a center of mass (CM) angle Θ_{CM} of $60.4 \pm 0.3^\circ$. Each supersonic beam was generated via a piezoelectric pulse valve, which was operated at a repetition rate of 60 Hz, a pulse width of 80 μs and peak voltage of -400 V . The neat 1,3-butadiene gas was triggered 90 μs prior to the methylidyne beam. Experiments with (partially) deuterated reactants were also conducted with methylidyne-d (CD) radical produced using bromoform-d (CDBr_3 , Aldrich Chemistry, 99.5%+) as a photodissociation precursor. The peak velocities and speed ratios of the reactants along with the corresponding collision energies and CM angles are summarized in Table 1.

The neutral reaction products entering the detector were first ionized by electron impact ionizer (80 eV),^[27] filtered according to their mass-to-charge ratios (m/z) by a quadrupole mass spectrometer (QMS, Extrel; QC 150) equipped with a 2.1 MHz oscillator, and ultimately detected by a Daly-type ion counter.^[28] The detector is housed within a triply differentially pumped chamber and rotatable in the plane defined by both reactant beams. Up to 7.2×10^5 time-of-flight (TOF) spectra were

collected at laboratory angles between $0^\circ \leq \Theta \leq 69^\circ$ with respect to the methylidyne beam ($\Theta = 0^\circ$). A forward-convolution routine was used to analyze the laboratory data, which is an iterative method exploiting user-defined center-of-mass (CM) translational energy $P(E_t)$ and angular $T(\theta)$ flux distributions; these functions are varied iteratively until an acceptable fit of the laboratory frame (LAB) TOF spectra and angular distributions are obtained.^[29,30] These functions define the reactive differential cross section $I(u, \theta) \sim P(u) \times T(\theta)$ with the center-of-mass velocity u . The error ranges of the $P(E_t)$ and $T(\theta)$ functions are determined within 1σ limits of the corresponding laboratory angular distribution while maintaining a good fit of the laboratory TOF spectra.

2.2. Computational

Geometries of the reactants, intermediates, transition states, and products of the $\text{CH} + 1,3\text{-butadiene}$ reaction accessing the C_5H_7 potential energy surface (PES) were optimized at the B3LYP/6-311G(d,p) level of theory^[31,32] and their vibrational frequencies were computed using the same method to evaluate zero-point vibrational energy corrections (ZPE) and to be utilized in rate constant calculations. Single-point energies were then refined using the explicitly-correlated coupled clusters CCSD(T)-F12 approach^[33,34] with Dunning's correlation-consistent cc-pVTZ-f12 basis set.^[35,36] The CCSD(T)-F12/cc-pVTZ-f12//B3LYP/6-311G(d,p)+ZPE(B3LYP/6-311G(d,p)) relative energies have been shown to be typically accurate within 4 kJ mol^{-1} or better.^[37] The GAUSSIAN 09^[38] and MOLPRO 2010^[36] program packages were used for the ab initio calculations. Rice-Ramsperger-Kassel-Marcus (RRKM) theory,^[39–41] was employed to compute energy-dependent rate constants of all unimolecular reaction steps on the C_5H_7 PES ensuing the initial association of the methylidyne radical with 1,3-butadiene. Here, rate constants were evaluated as functions of the available internal energy of each intermediate or transition state within the harmonic approximation using B3LYP/6-311G(d,p) frequencies and employing our in-house code Unimol.^[42] Unimol is an updated version of our previous software code on energy dependent RRKM calculations of rate constants for multiwell and multi-channel unimolecular reactions under single-collision conditions and for solving a system of first-order kinetic equations.^[43] Unimol automatically processes GAUSSIAN 09 log files to compute numbers of states for transition states and densities of states for local minima employing the direct count method. The internal energy is assumed to be equal to the sum of the collision energy and the chemical activation energy, that is, negative of the relative energy of a species with respect to the reactants. Only one energy level is considered throughout as at a zero-pressure limit corresponding to crossed molecular beams conditions. RRKM rate constants are then used to compute product branching ratios by solving first-order kinetic equations within steady-state approximation.^[42,43]

Table 1. Peak velocities (v_p) and speed ratios (S) of the methylidyne (CH), methylidyne-d (CD) beams, 1,3-butadiene (C_4H_6), 1,3-butadiene-d₆ (C_4D_6), 1,3-butadiene-1,1,4,4-d₄ ($\text{C}_4\text{H}_2\text{D}_4$) along with the corresponding collision energies (E_c) and center-of-mass angles (Θ_{CM}) for each reactive scattering experiment.

Beam	v_p [m s^{-1}]	S	E_c [kJ mol^{-1}]	Θ_{CM} [degree]
$\text{CH} (\text{X}^2\Pi)$	1836 ± 15	11.6 ± 0.9		
$\text{C}_4\text{H}_6 (\text{X}^1\text{A}_g)$	777 ± 12	9.5 ± 0.3	20.8 ± 0.4	60.4 ± 0.3
$\text{C}_4\text{D}_6 (\text{X}^1\text{A}_g)$	750 ± 10	8.0 ± 0.2	21.0 ± 0.4	62.1 ± 0.3
$\text{CD} (\text{X}^2\Pi)$	1816 ± 15	13.1 ± 0.8		
$\text{C}_4\text{H}_6 (\text{X}^1\text{A}_g)$	777 ± 12	9.5 ± 0.3	21.7 ± 0.4	58.8 ± 0.3
$\text{CD}_2\text{CHCHCD}_2 (\text{X}^1\text{A}_g)$	760 ± 10	5.9 ± 0.2	21.9 ± 0.4	60.0 ± 0.3

3. Results

3.1. Laboratory Frame

For the reaction of the methylidyne radical (CH ; 13 amu) with 1,3-butadiene ($\text{CH}_2\text{CHCHCH}_2$; 54 amu), reactive scattering signal was detected at mass to charge ratios (m/z) of 67 (${}^{13}\text{CC}_4\text{H}_6^+$), 66 (C_5H_6^+), and 65 (C_5H_5^+). These TOF spectra depict identical pattern after scaling suggesting that ion counts $m/z=67$, 66, and 65 originate from the same reaction channel, i.e. the formation of the heavy reaction product C_5H_6 (66 amu) along with atomic H (1 amu) emission. Therefore, signal at $m/z=65$ (C_5H_5^+) arose from dissociative electron impact ionization of the $m/z=66$ (C_5H_6^+) parent product, whereas $m/z=67$ (${}^{13}\text{CC}_4\text{H}_6^+$) represented the natural distribution of carbon atom isotopes leading to ${}^{13}\text{CC}_4\text{H}_6$ with signal collected at level of 5 ± 2 %. Since the ion counts of the parent ion $m/z=66$ (C_5H_6^+) are collected only at a level of 39 ± 4 % compared to the fragment ion $m/z=65$ (C_5H_5^+), the TOF spectra were recorded at the best signal-to-noise ratio at $m/z=65$ (C_5H_5^+). The resulting TOFs were then normalized with respect to the center-of-mass angle and integrated to obtain the laboratory angular distribution (LAB; Figure 1). The LAB is nearly symmetric around the center-of-mass angle (Θ_{CM}) and spans at least 27° in the laboratory frame. This result indicates that the reaction of the methylidyne radical with 1,3-butadiene likely proceeds via indirect scattering dynamics through C_5H_7 reaction intermediate(s) ultimately dissociating to the heavy product C_5H_6 by emitting atomic hydrogen.

To trace the position(s) of the hydrogen atom emission, the reactions of the methylidyne-d radical (CD ; 14 amu) with 1,3-butadiene ($\text{CH}_2\text{CHCHCH}_2$; 54 amu) and of the methylidyne radical (CH ; 13 amu) with 1,3-butadiene-d₆ ($\text{CD}_2\text{CDCDCD}_2$; 60 amu) and 1,3-butadiene-1,1,4,4-d₄ ($\text{CD}_2\text{CHCHCD}_2$; 58 amu) were also studied (Scheme 2). First, the reaction of methylidyne-d (CD ; 14 amu) with 1,3-butadiene ($\text{CH}_2\text{CHCHCH}_2$; 54 amu) was studied (Scheme 2 (b)) to probe the hydrogen atom loss channel. TOFs were collected at $m/z=67$ ($\text{C}_5\text{H}_5\text{D}^+$) and $m/z=66$ ($\text{C}_5\text{H}_6^+/\text{C}_5\text{H}_4\text{D}^+$) at the Θ_{CM} of 58.8° ; signal at both m/z ratios was observed with signal at $m/z=67$ ($\text{C}_5\text{H}_5\text{D}^+$) collected at a level of 77 ± 2 % of $m/z=66$ ($\text{C}_5\text{H}_6^+/\text{C}_5\text{H}_4\text{D}^+$) (Figure 2). We can conclude that signal at $m/z=67$ ($\text{C}_5\text{H}_5\text{D}^+$) can only be attributed to the atomic hydrogen loss channel, i.e. hydrogen must be emitted from the 1,3-butadiene reactant. Signal at $m/z=m/z=66$ ($\text{C}_5\text{H}_6^+/\text{C}_5\text{H}_4\text{D}^+$) is not unique as it can originate from the dissociative electron impact ionization of the $m/z=67$ ($\text{C}_5\text{H}_5\text{D}^+$) product and also from the atomic deuterium loss pathway.

To verify this conclusion, we performed the reaction of the methylidyne radical (CH ; 13 amu) with 1,3-butadiene-d₆ ($\text{CD}_2\text{CDCDCD}_2$; 60 amu) (Scheme 2 (c)). Atomic hydrogen and atomic deuterium emission channels were probed at mass to charge ratios (m/z) of 72 (C_5D_6^+) and 71 (C_5HD_5^+) (Figure 2), respectively. Note that ions at $m/z=72$ (C_5D_6^+) cannot fragment to $m/z=71$ (C_5HD_5^+). Compared with the signal at $m/z=71$ (C_5HD_5^+), ion counts at $m/z=72$ (C_5D_6^+) are hardly visible with its signal intensity accounting for 6 ± 1 % with respect to $m/z=$

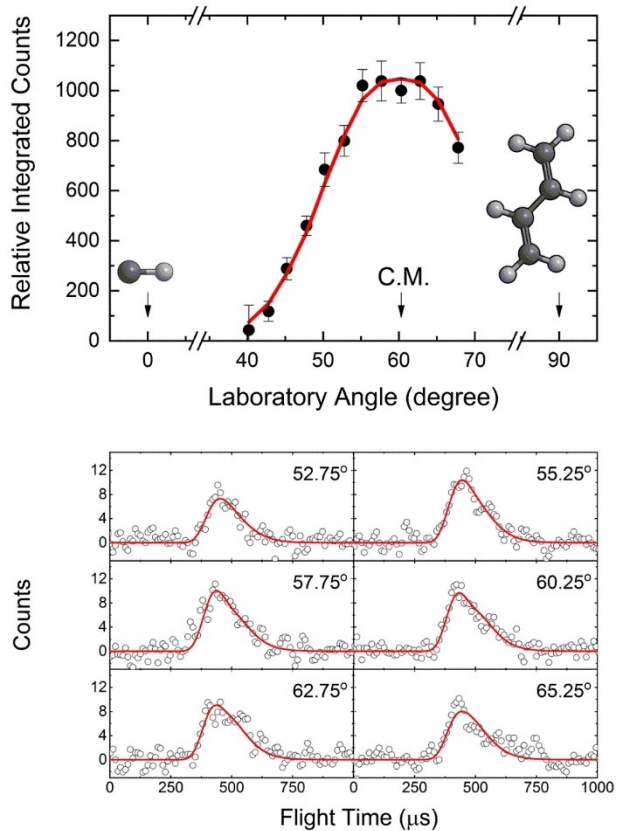


Figure 1. Laboratory angular distribution (top) and time-of-flight (TOF) spectra (bottom) recorded at mass-to-charge ratio (m/z) of 65 for the reaction of the methylidyne radical (CH ; $\text{C}_{\infty\text{v}}$; X^{II}) with 1,3-butadiene ($\text{CH}_2\text{CHCHCH}_2$; $\text{C}_{2\text{h}}$; X^{A_g}). The directions of the methylidyne radical and 1,3-butadiene beams are defined as 0° and 90° , respectively. The red solid lines represent the best-fit derived from center-of-mass functions depicted in Figure 3 with black circles defining the experimental data.

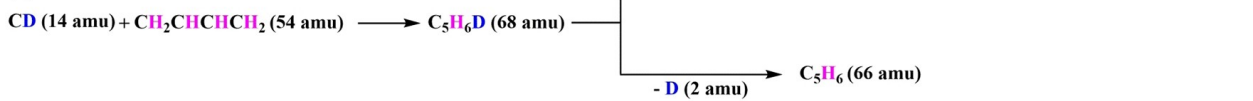
71 (C_5HD_5^+); this indicates that only atomic deuterium emission is present; signal at $m/z=72$ can be linked to ${}^{13}\text{CC}_4\text{H}_2\text{D}_4^+$. Therefore, the consistent experimental results for the reactions of methylidyne-d (CD ; 14 amu) with 1,3-butadiene ($\text{CH}_2\text{CHCHCH}_2$; 54 amu) and methylidyne radical (CH ; 13 amu) with 1,3-butadiene-d₆ ($\text{CD}_2\text{CDCDCD}_2$; 60 amu) suggest that for the methylidyne (CH)-1,3-butadiene ($\text{CH}_2\text{CHCHCH}_2$) system, the atomic hydrogen loss originates from the 1,3-butadiene reactant.

We further carried out the reaction of the methylidyne-d radical (CD ; 14 amu) with 1,3-butadiene-1,1,4,4-d₄ ($\text{CD}_2\text{CHCHCD}_2$; 58 amu) (Scheme 2 (d)). Only atomic hydrogen loss channel with signals at $m/z=71$ (C_5HD_5^+) is unique and hence was collected (Figure 2). After 11.5 hours TOF accumulation, the peak at $m/z=71$ (C_5HD_5^+) is barely visible and can be easily accounted for by ${}^{13}\text{CC}_4\text{H}_2\text{D}_4^+$. These results suggest that atomic hydrogen is not emitted from the C2/C3 positions of 1,3-butadiene. In summary, for the reaction of the methylidyne radical (CH ; 13 amu) with 1,3-butadiene ($\text{CH}_2\text{CHCHCH}_2$), the

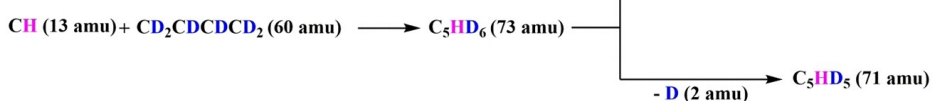
(a)



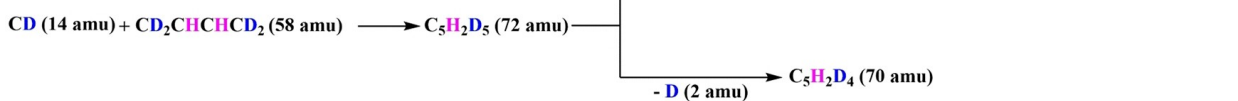
(b)



(c)



(d)



Scheme 2. Reaction schematics for the reactions of (a) methylidyne (CH) with 1,3-butadiene ($\text{CH}_2\text{CHCHCH}_2$), (b) methylidyne-d (CD) with 1,3-butadiene ($\text{CH}_2\text{CHCHCH}_2$), (c) methylidyne (CH) with 1,3-butadiene-d₆ ($\text{CD}_2\text{CDCDCD}_2$), and (d) methylidyne-d (CD) with 1,3-butadiene-1,1,4,4-d₄ ($\text{CD}_2\text{CHCHCD}_2$), leading to H– and D– loss products. Successive dissociative electron impact processes of the parent ions are represented in italics.

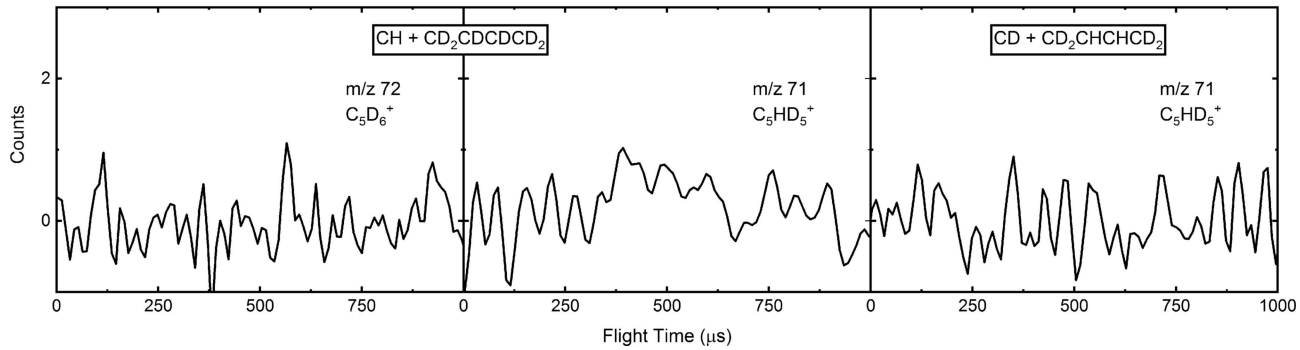
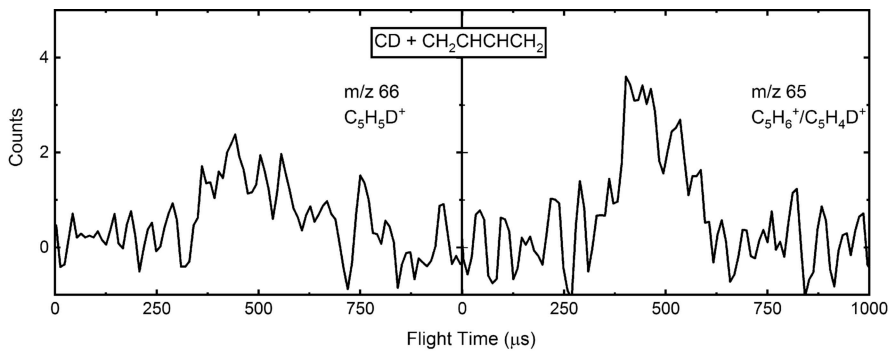


Figure 2. Time-of-flight (TOF) spectra for the reaction of the methylidyne-d (CD) with 1,3-butadiene ($\text{CH}_2\text{CHCHCH}_2$), methylidyne (CH) with 1,3-butadiene-d₆ ($\text{CD}_2\text{CDCDCD}_2$), and methylidyne-d (CD) with 1,3-butadiene-1,1,4,4-d₄ ($\text{CD}_2\text{CHCHCD}_2$).

atomic hydrogen emission channel originates predominantly from the terminal CH_2 group of the 1,3-butadiene reactant.

3.2. Center-of-Mass Frame

For the reaction of the methylidyne radical (CH ; 13 amu) with 1,3-butadiene ($\text{CH}_2\text{CHCHCH}_2$; 54 amu), the best-fit TOF spectra (Figure 1), LAB angular distribution (Figure 1), and corresponding CM translational energy $P(E_T)$ and angular $T(\theta)$ distributions (Figure 3) are attained via a single reaction channel accounting for C_5H_6 product(s) along with atomic hydrogen; the hatched areas of the $P(E_T)$ and $T(\theta)$ were determined within the 1σ error limits of the LAB angular distribution. According to the principle of conservation of energy, the maximum energy E_{\max} of the CM translational energy distribution $P(E_T)$ (Figure 3) can be linked with the collision energy (E_c) and the reaction energy (Δ_rG) via $E_{\max} = E_c - \Delta_rG$ for those molecules born without internal excitation. The $P(E_T)$ terminates at $140 \pm 42 \text{ kJ mol}^{-1}$ suggesting a reaction energy of $-119 \pm 42 \text{ kJ mol}^{-1}$ to form C_5H_6 isomers along with atomic hydrogen emission. The distribution maximum of $P(E_T)$ is located at $16 \pm 5 \text{ kJ mol}^{-1}$ with an average

translational energy of the products derived to be $34 \pm 9 \text{ kJ mol}^{-1}$; this reveals that only $24 \pm 6\%$ of the available energy is released into the product translation degrees of freedom. These findings suggest indirect reactive scattering dynamics leading to C_5H_6 isomer(s) via C_5H_7 intermediate(s).^[44] Further, $T(\theta)$ carries non-zero intensity over the complete angular range indicating that the product is formed via indirect scattering dynamics via activated C_5H_7 complex(es); the forward-backward symmetry of $T(\theta)$ implies that the lifetime of the intermediate C_5H_7 is longer than its rotational period(s).^[45]

4. Discussion

We now combine our experimental data with electronic structure and statistical calculations to reveal the underlying reaction mechanism(s) leading to C_5H_6 formation (Figures 4–8, Figures S1–S4; Table 2). In principle, the methylidyne radical (CH) can add to a carbon atom, add across the carbon–carbon double bond, and may insert into various C–H bonds or the carbon–carbon single bond of 1,3-butadiene; therefore the doublet C_5H_7 potential energy surface (PES) was explored systematically by connecting the methylidyne radical plus 1,3-butadiene reactants in multiple entrance channels eventually via 38 C_5H_7 intermediates (i1–i38) and 91 transition states to the atomic hydrogen loss C_5H_6 products (p1–p16) (Figures 4–7). Due to this complexity, the complete PES is segmented into four portions: (1) products p1–p6 produced by methylidyne radical addition to the terminal carbon atom, the carbon–carbon double bond, and insertion into to the terminal C–H bond or carbon–carbon single bond of 1,3-butadiene via intermediates i1–i13, i16, i17 (Figure 4), (2) products p7–p11 resulting from the same initial channels involving intermediates

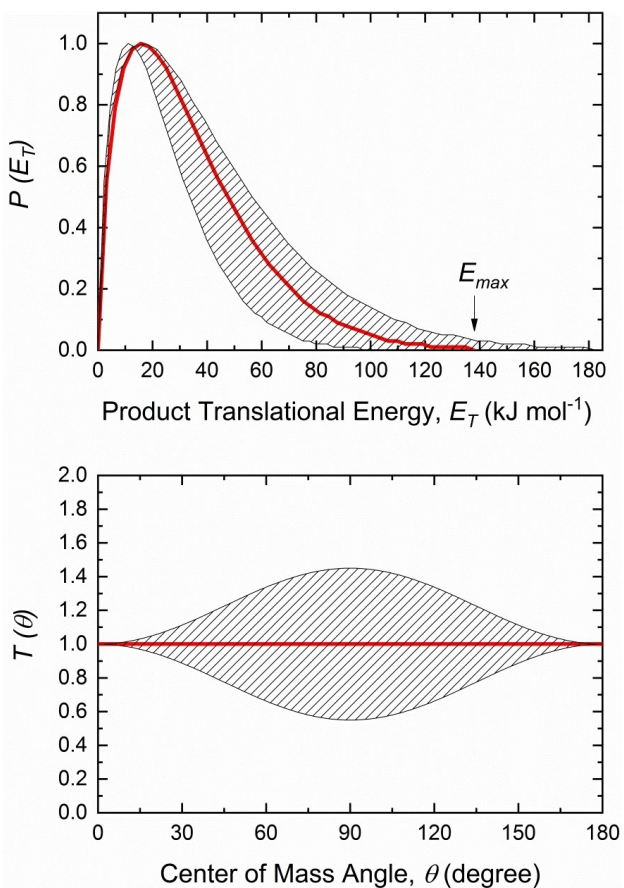


Figure 3. Best-fit center-of-mass translational energy ($P(E_T)$, upper) and angular ($T(\theta)$, lower) flux distributions of the reaction of the methylidyne radical with 1,3-butadiene to form C_5H_6 molecule(s) plus atomic hydrogen. The red lines reveal the best fits; the shaded areas delimit the acceptable upper and lower error limits. E_{\max} defines the maximum translational energy.

Table 2. Statistical branching ratios (%) for the reaction of the methylidyne (CH) radical with 1,3-butadiene ($\text{CH}_2\text{CHCHCH}_2$) at collision energy $E_c = 20.8 \text{ kJ mol}^{-1}$ ^[a]

Initial intermediate	i1	i2	i3	i4
	100	100	100	100
p1	76.2	76.0	76.3	76.3
p2	3.8	3.8	3.8	3.8
p3	4.1	4.0	4.0	4.0
p4	0.0	0.0	0.0	0.0
p5	0.0	0.0	0.0	0.0
p6	0.0	0.1	0.0	0.0
p7	0.0	0.0	0.0	0.0
p8	0.3	0.3	0.3	0.3
p9	15.4	15.3	15.4	15.4
p10	0.1	0.1	0.1	0.1
p11	0.0	0.0	0.0	0.0
p12	0.0	0.0	0.0	0.0
p13	0.2	0.1	0.1	0.1
p14	0.0	0.2	0.0	0.0
p15	0.0	0.0	0.0	0.0
p16	0.0	0.0	0.0	0.0

[a] Here, p1–p16 are cyclopentadiene, trans-1,2,4-pentatriene, cis-1,2,4-pentatriene, 4-penten-1-yne, 1-vinyl-cyclopropene, cis-3-vinyl-cyclopropene, 1-penten-4-yne, 1-penten-3-yne, (Z)-3-penten-1-yne, 1,2,3-pentatriene, trans-3-vinyl-cyclopropene, 1-methyl-1,3-cyclobutadiene, 3-methylene-cyclobutene, cyclopropylacetylene, 3-penten-1-yne, and 3-ethylidene-cyclopropene.

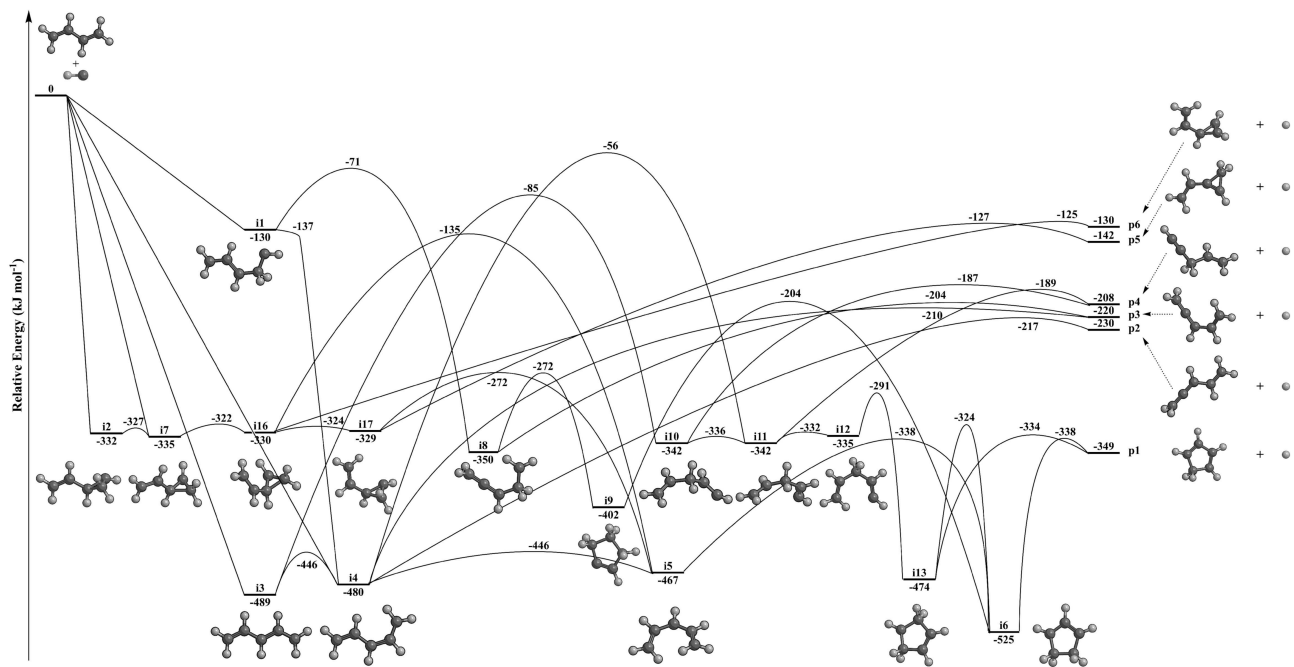


Figure 4. Portion of the C_5H_7 potential energy surface (PES) leading to $p1-p6$.

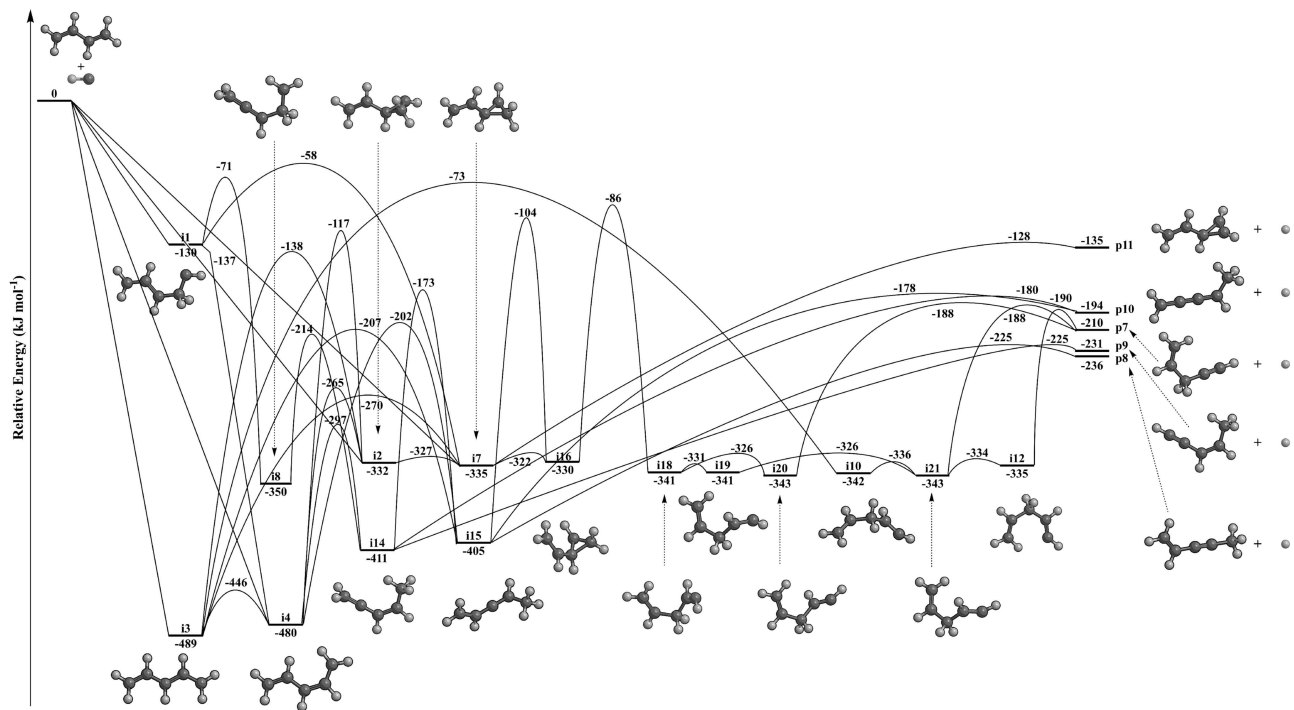
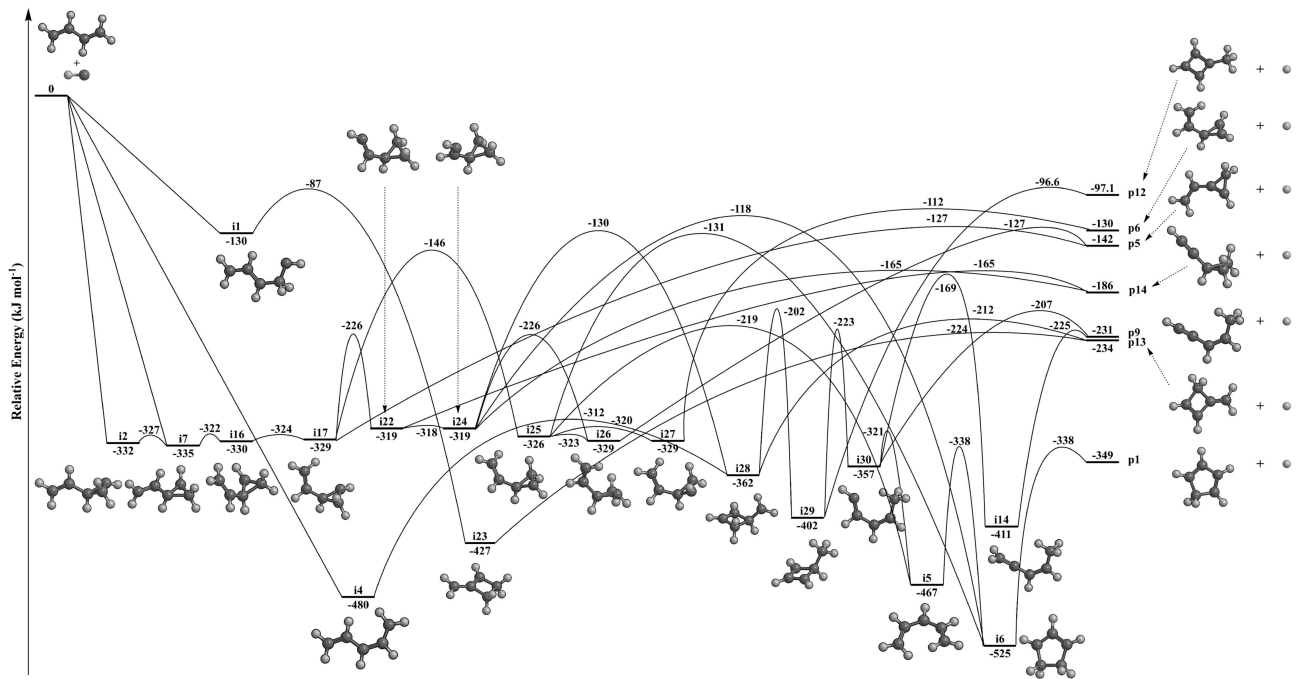
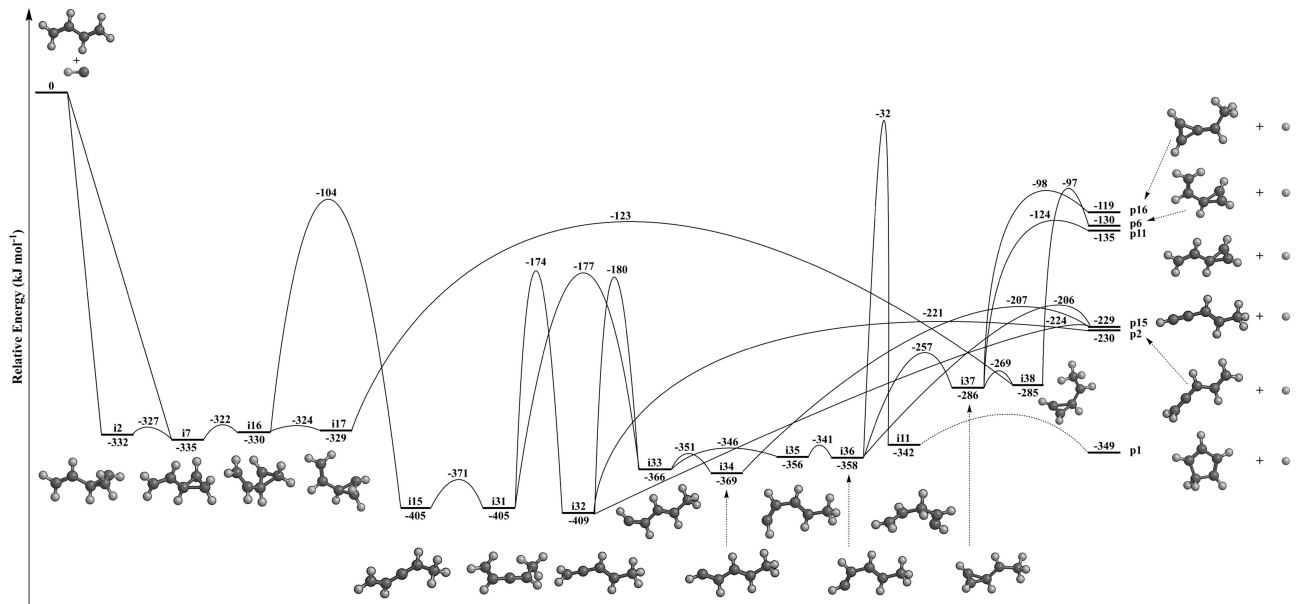


Figure 5. Portion of the C_5H_7 PES leading to $p7-p11$.

i1–i4, i7, i8, i10, i12, i14–i16, i18–i21 (Figure 5), (3) products $p1, p5, p6, p9, p12–p14$ originating from CH addition to the terminal carbon atom and the carbon–carbon double bond of 1,3-butadiene via $i1, i2, i5–i7, i14, i16, i17, i22–i30$ (Figure 6), and (4) products $p1, p2, p6, p11, p15, p16$ stemming from methylidyne radical addition to the carbon–carbon double

bond of 1,3-butadiene through intermediates $i2, i7, i11, i15–i17, i31–i38$ (Figure 7); Figures S1–S4 trace the hydrogen atom loss in the methylidyne-1,3-butadiene reaction for the reactions involving partially deuterated reactants. Considering the overall reaction energies, cyclopentadiene ($p1$), trans-1,2,4-pentatriene ($p2$), cis-1,2,4-pentatriene ($p3$), 4-penten-1-yne ($p4$), 1-vinyl-

Figure 6. Portion of the C_5H_7 PES leading to **p1**, **p5**, **p6**, **p9**, **p12–p14**.Figure 7. Portion of the C_5H_7 PES leading to **p1**, **p2**, **p6**, **p11**, **p15**, **p16**.

cyclopropene (**p5**), cis-3-vinyl-cyclopropene (**p6**), 1-penten-4-yne (**p7**), 1-penten-3-yne (**p8**), (Z)-3-penten-1-yne (**p9**), 1,2,3-pentatriene (**p10**), trans-3-vinyl-cyclopropene (**p11**), 1-methyl-1,3-cyclobutadiene (**p12**), 3-methylene-cyclobutene (**p13**), cyclopropylacetylene (**p14**), 3-penten-1-yne (**p15**), and 3-ethylidene-cyclopropene (**p16**) isomers can be formed along with the atomic hydrogen with computed reaction energies of -349 , -230 , -220 , -208 , -142 , -130 , -210 , -236 , -231 , -194 , -135 , -97 , -234 , -186 , -229 , and -119 kJ mol^{-1} ,

respectively. These calculated reaction energies are expected to be accurate within 4 kJ mol^{-1} . The computed reaction energy for the formation of 1-vinyl-cyclopropene (**p5**), cis-3-vinyl-cyclopropene (**p6**), trans-3-vinyl-cyclopropene (**p11**), 1-methyl-1,3-cyclobutadiene (**p12**), and 3-ethylidene-cyclopropene (**p16**) plus atomic hydrogen ranging between -142 and -97 kJ mol^{-1} correlate with our experimentally determined reaction energy of $-119 \pm 42\text{ kJ mol}^{-1}$.

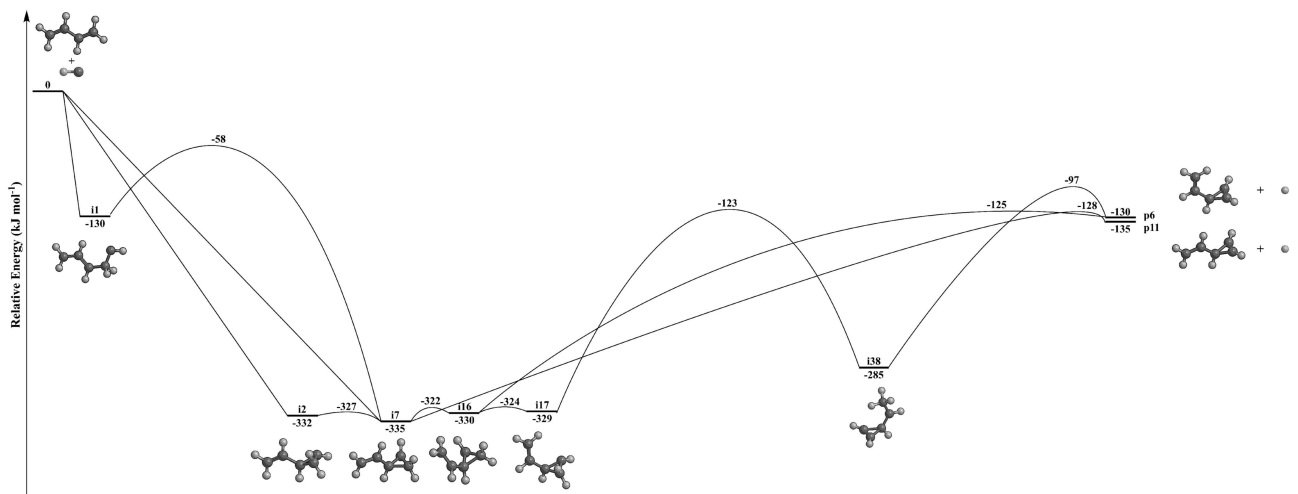


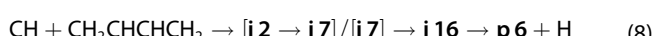
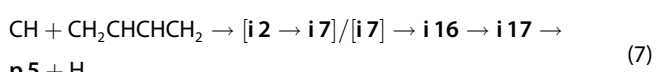
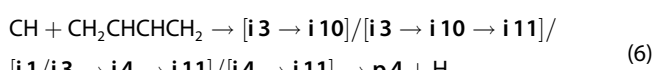
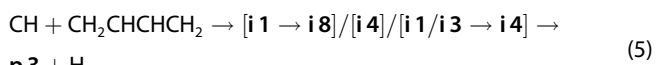
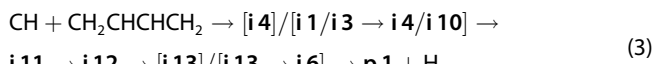
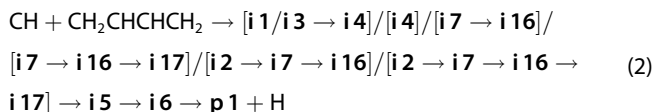
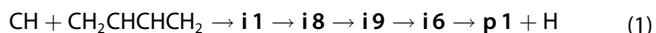
Figure 8. Reduced C_5H_7 PES leading to **p6, p11**.

4.1. CH addition to the terminal carbon atom, the carbon–carbon double bond, and insertion into terminal C–H and carbon–carbon single bond of 1,3-butadiene leading to products **p1–p6** via intermediates **i1–i13, i16, i17** (Figure 4)

The methylidyne radical can add barrierlessly to the terminal carbon atom of 1,3-butadiene, to the carbon–carbon double bond, and may insert into the terminal C–H bond or carbon–carbon single bond of 1,3-butadiene forming the initial adduct **i1**, **i2** or **i7**, and **i3** or **i4**, respectively. A 1,2-H migration from the former terminal CH_2 group of 1,3-butadiene to the newly added CH moiety in **i1** connects this initial adduct with **i4**. A low barrier of 2.6 kJ mol^{-1} exists between **i1** and **i4** at the B3LYP level of theory, however, the energy of the corresponding transition state is lower than that of **i1** after refinement at the CCSD(T)-F12 level. This means that **i1** could be only a metastable structure. Nevertheless, we keep **i1** in our consideration because this metastable structure can serve as pivot on the pathways to the **i7**, **i8**, and **i23** intermediates discussed below. For instance, a 1,4-hydrogen atom migration from the CH_2CH group to the terminal CH moiety in **i1** leads to **i8**. The cis-1,2,4-pentatriene (**p3**) product can be formed via hydrogen atom emission from the non-terminal CH_2 group in **i8** via a tight exit transition state lying 16 kJ mol^{-1} above the separated products. Ring closure in **i8** results in a cyclic intermediate **i9**; hydrogen migration from the CH_2 group to the adjacent bare carbon atom in **i9** leads to **i6**. The initial adducts **i2** and **i7** can easily undergo rotational rearrangements to the other conformers **i16** and **i17**. Intermediate **i16** can eliminate a hydrogen atom from the CH_2 group of the $CH \cdot CHCH_2$ moiety yielding cis-3-vinyl-cyclopropene (**p6**) via a loose exit transition state located only 5 kJ mol^{-1} above the separated products. Intermediates **i16** and **i17** are connected via a low barrier of only 6 kJ mol^{-1} above **i16**; the decomposition of the later forms 1-vinyl-cyclopropene (**p5**) via atomic hydrogen emission from the CH group of the $CH \cdot CHCH_2$ moiety in **i17**. Intermediate **i17** can also open its three-member ring to form an acyclic intermediate

i5. The CH_2 to CH hydrogen atom shift in the three-member ring accompanied with the ring opening in intermediate **i16** leads to **i5** too; a five-member ring closure may ultimately give rise to intermediate **i6**. Intermediate **i3** can isomerize to **i4** by rotation around a carbon–carbon bond via a low-lying transition state of 43 kJ mol^{-1} above **i3**. Meanwhile, 1,3-hydrogen migration in **i3** connects it to intermediate **i10** via a high barrier located at 404 kJ mol^{-1} above **i3**. Different conformers **i10** and **i11** are connected via a low-lying rotational transition state of only 6 kJ mol^{-1} above **i10**. Both isomers may eliminate atomic hydrogen from the non-terminal CH group of the terminal $CHCH$ moiety yielding 4-penten-1-yne (**p4**). The intermediate **i11** can isomerize to yet another conformer **i12** by rotation around a C–C bond, followed by ring closure to form **i13**, and a 1,2-H shift in the latter produces **i6**. An atomic hydrogen emission from any CH_2 group of **i13** and **i6** yields cyclopentadiene (**p1**) via exit transition states lying 15 and 11 kJ mol^{-1} above the separated products, respectively. The trans-1,2,4-pentatriene (**p2**) and cis-1,2,4-pentatriene (**p3**) products can be formed via atomic hydrogen emissions from the CH groups of terminal $CHCH_2$ moieties of **i4**. In brief, **p1** can be formed via pathways (1)–(3), which start with intermediates **i1–i4** and **i7**. Products **p2** and **p4**, can be accessed via pathways (4), (6), respectively, with atomic hydrogen elimination originating from the CH moiety of the 1,3-butadiene reactant if **i3** is formed by methylidyne insertion into the single C–C bond of 1,3-butadiene or by hydrogen atom loss from the CH_2 group of 1,3-butadiene if **i3** is produced by the CH insertion into the terminal C–H bond of 1,3-butadiene. Product **p5** forms via pathway (7) by hydrogen elimination from the CH group of 1,3-butadiene. Product **p3** is produced via pathway (5) with the hydrogen atom loss originating from the CH and/or CH_2 moiety of the 1,3-butadiene reactant. Product **p6** is formed through pathway (8) with the hydrogen eliminated solely from the CH_2 moiety of 1,3-butadiene reactant. Considering only the experimentally derived reaction energy of $-119 \pm 42\text{ kJ mol}^{-1}$, 1-vinyl-cyclopropene (**p5**) and cis-3-vinyl-cyclopropene (**p6**) with

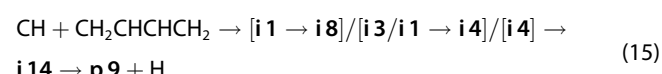
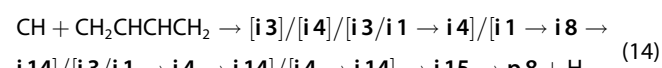
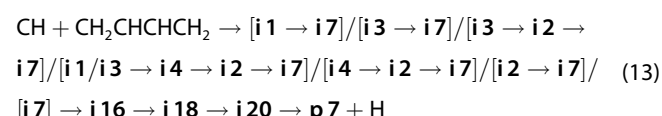
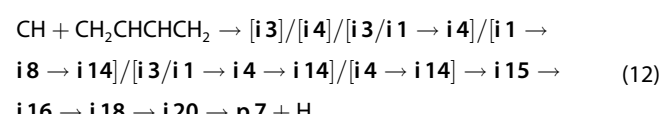
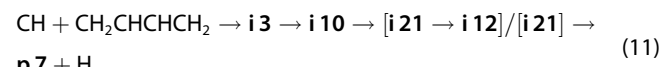
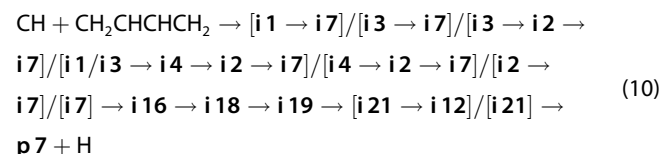
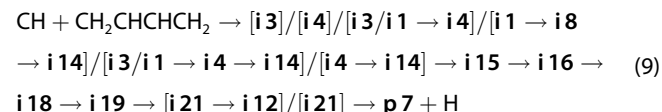
reaction energies of -142 and -130 kJ mol^{-1} are the most likely reaction products. Accounting for the results of our isotopic substitution experiments, i.e. the hydrogen atom emission originates solely from the CH_2 group of the 1,3-butadiene reactant, we can exclude the formation of 1-ethenyl-cyclopropene (**p5**) since this would require a hydrogen elimination from the CH moiety of the 1,3-butadiene reactant. Therefore, *cis*-3-vinyl-cyclopropene (**p6**) is the product that can be formed via pathway (8) under our experimental conditions.

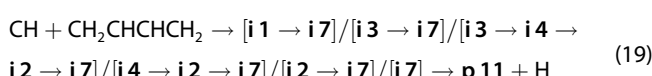
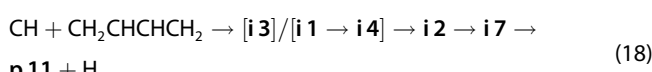
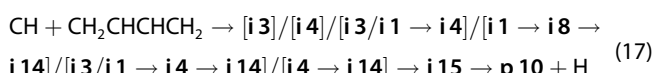
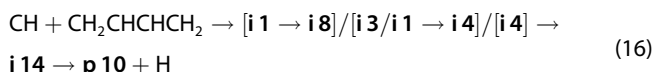


4.2. CH addition to the terminal carbon atom, the carbon–carbon double bond, and insertion into terminal C–H or carbon–carbon single bonds of 1,3-butadiene leading to products **p7**–**p11** via intermediates **i1**–**i4**, **i7**, **i8**, **i10**, **i12**, **i14**–**i16**, **i18**–**i21** (Figure 5)

Intermediates **i3** and **i4** can isomerize to **i7** and **i2** via three-member ring closure barriers of 219 and 215 kJ mol^{-1} ; if the ring closure are accompanied with an H shift the barriers increase to 351 and 363 kJ mol^{-1} , respectively. The ring closure in **i1** leads to **i7**, which connects to **i2** via a low-lying rotational transition state of 5 kJ mol^{-1} above **i2**. The trans-3-vinyl-cyclopropene (**p11**) product can be formed via atomic hydrogen emission from the CH_2 group of the $\text{CH}\cdot\text{CHCH}_2$ moiety in **i7**. The 1,3-, 1,4-, and 1,2-hydrogen migrations in **i3**, **i4**, and **i8** results in intermediates **i14** and **i15**. The 1,2,3-pentatriene (**p10**) product can be accessed via atomic hydrogen emission from the CH group of **i14** and **i15** via tight exit transition states residing 14 and 16 kJ mol^{-1} above the separated products, respectively. A hydrogen atom emitted from the CH_2 group of **i14** yielding (*Z*)-3-penten-1-yne (**p9**) via a loose exit transition state residing 6 kJ mol^{-1} above the separated products. The 1-penten-3-yne (**p8**) product can also be accessed via atomic hydrogen emission from the CH group in the CHCH_3 moiety of **i15**.

Hydrogen migration occurring together with the ring opening in **i16** leads to the group of conformers **i18**–**i21**, **i10**, and **i12**, and eventually to 1-penten-4-yne (**p7**) via atomic hydrogen emission from the CH group of **i20**, **i21**, and **i12**. In brief, **p7**–**p11** can be formed via pathways (9)–(19). Products **p7**, **p10** and **p11** can be accessed via hydrogen emission from both reactants, while products **p8** and **p9** can only be accessed through hydrogen emission from 1,3-butadiene reactant. Considering the experimentally derived reaction energy of $-119 \pm 42 \text{ kJ mol}^{-1}$, trans-3-vinyl-cyclopropene (**p11**) with an overall reaction energy of -135 kJ mol^{-1} is the most likely product among products **p7**–**p11**. When **i3** and/or **i4** are formed via methylidyne radical insertion into a terminal C–H bond followed by the isomerization between **i3**/**i4** to **i7**/**i2** via high barriers of $219/215 \text{ kJ mol}^{-1}$, formation of product **p11** can occur by atomic hydrogen emission either from 1,3-butadiene or CH reactants. Therefore, we can rule out pathway (18). The pathway (19), where **i3** and/or **i4** are formed via methylidyne radical (CH) insertion into C–C single bond of 1,3-butadiene and isomerization between **i4** to **i2** via a barrier of 215 kJ mol^{-1} , leading to **p11** can be accessed via hydrogen emission from the CH_2 moiety in 1,3-butadiene reactant, which is consistent with the results of our isotope substitution experiments. Therefore, we can conclude that the formation of trans-3-vinyl-cyclopropene (**p11**) via pathway (19) is feasible under our experimental conditions.

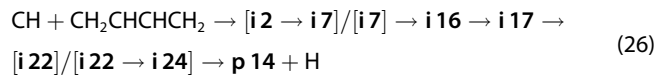
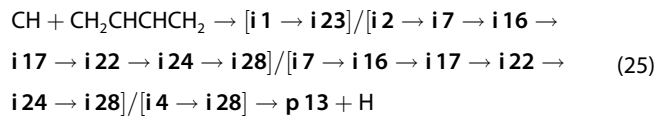
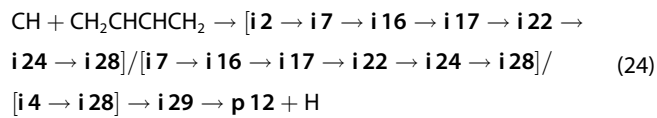
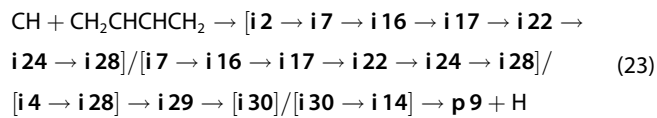
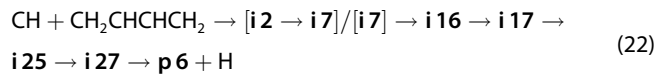
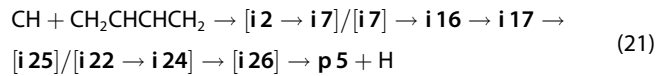
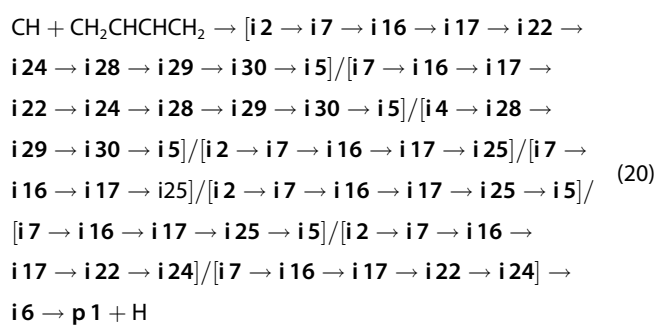




4.3. CH addition to the terminal carbon atom, and the carbon–carbon double bond of 1,3-butadiene leading to products p1, p5, p6, p9, p12–p14 via intermediates i1, i2, i5–i7, i14, i16, i17, i22–i30 (Figure 6)

1,4-H shift accompanied with ring closure in i1 leads to the four-member cyclic intermediate i23. The product 3-methylene-cyclobutene (p13) can be formed via atomic hydrogen emission from the CH₂ group of i23 via a loose exit transition state lying 10 kJ mol⁻¹ above the separated products. Intermediate i17 can isomerize to i22 and i25 via barriers of 103 and 183 kJ mol⁻¹, respectively. Intermediate i22 can isomerize to i24 via a low-lying rotational barrier of just 1 kJ mol⁻¹. The cyclopropylacetylene (p14) product is accessible via atomic hydrogen emission both from i22 and i24, respectively. 1,4-Hydrogen migration in i24 leads to i26. Both intermediates i25 and i26 are connected via a low-lying rotational barrier of just 3 kJ mol⁻¹ above i25. The 1-vinyl-cyclopropene (p5) product can be formed via atomic hydrogen emission from the CH group of the cCH·CHCH₂ moiety in i26. The hydrogen atom emission from the CH₂ group of cCHCHCH₂ moiety in i27, which represents another conformer of i25, yields cis-3-vinyl-cyclopropene (p6). The isomerization of the three-member cyclic i24 to the four-member cyclic i28 can proceed via a barrier of 189 kJ mol⁻¹ above i24. Intermediate i28 can form by four-member ring closure in i4. The 3-methylene-cyclobutene (p13) product might be formed via atomic hydrogen emission from i28. The latter can also isomerize to i29; the 1-methyl-1,3-cyclobutadiene (p12) product can also be formed through atomic hydrogen emission from the CH group of the CHCH₃ moiety of i29 via a loose exit transition state lying 0.5 kJ mol⁻¹ above the separated products. Ring opening in i29 leads to i30 followed by isomerization to i14. The (Z)-3-penten-1-yne (p9) product can be formed via hydrogen atom emission of i30 and i14 via a tight and loose exit transition state lying 24 and 6 kJ mol⁻¹ above the product for i30 and i14, respectively. The ring closure of i5 and isomerization from the three-member cyclic intermediates i24 and i25 both lead to a five-membered cyclic intermediate i6 where i25 can also directly ring-open to i5. The cyclopentadiene (p1) product could be produced via atomic hydrogen emission from the CH₂ group of i6 via a loose exit transition state lying 11 kJ mol⁻¹ above the separated products. In brief, p1, p5, p6, p9, and p12–p14 can be formed via pathway (20)–(26), respectively. Considering the experimentally

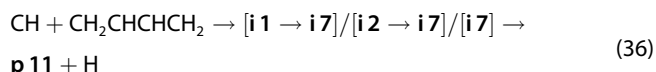
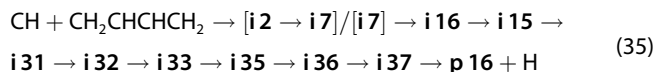
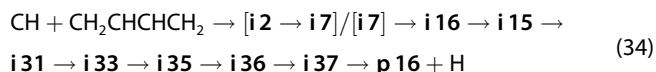
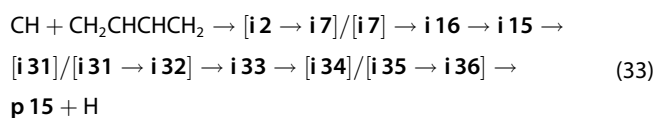
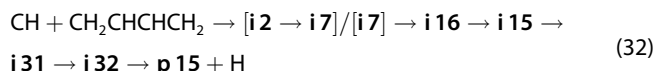
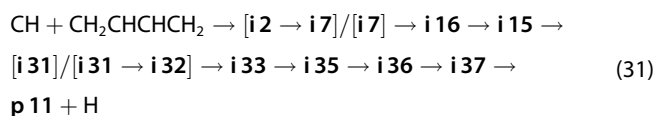
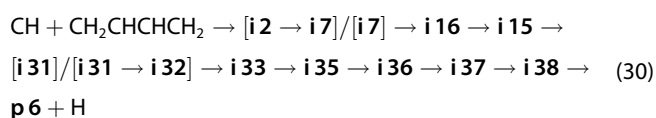
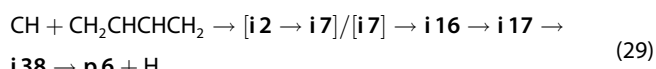
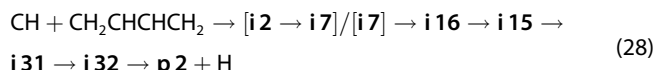
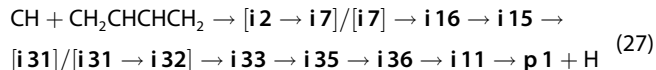
derived reaction energy of -119 ± 42 kJ mol⁻¹, 1-vinyl-cyclopropene (p5), cis-3-vinyl-cyclopropene (p6) and 1-methyl-1,3-cyclobutadiene (p12) with reaction energies of -142 , -130 and -97.1 kJ mol⁻¹ are the most likely products. However, the formation of p5 can only be accessed via hydrogen emission from the CH moiety of 1,3-butadiene reactant; for the cis-3-vinyl-cyclopropene (p6) and 1-methyl-1,3-cyclobutadiene (p12) products formed via the pathways described in this section, the hydrogen loss may originate not only from the CH₂ group of 1,3-butadiene, but also from the methylidyne (CH) radical reactant and the CH moiety of 1,3-butadiene reactant, respectively; this is inconsistent with the results of our isotopic substitution experiments. Therefore, we can conclude that pathways (20)–(26) are likely not open under our experimental conditions.



4.4. CH addition to the carbon–carbon double bond of 1,3-butadiene leading to products p₁, p₂, p₆, p₁₁, p₁₅, p₁₆ via intermediates i₂, i₇, i₁₁, i₁₅–i₁₇, i₃₁–i₃₈ (Figure 7)

Hydrogen atom shift together with the three-member ring opening in i₁₆ forms i₁₅. Further, the intermediates i₃₁ and i₁₅ are connected via a low-lying rotational transition state located at 34 kJ mol⁻¹ above i₁₅. The 1,2- and 1,3-hydrogen migrations in i₃₁ lead to i₃₂ and i₃₃, respectively. The trans-1,2,4-pentatriene (p₂) product can be formed via atomic hydrogen emission from the CH₃ group in i₃₂ via a loose exit transition state lying 9 kJ mol⁻¹ above the separated products. The 3-penten-1-yne (p₁₅) product can be accessed via hydrogen atom emitted from the terminal CH₂ group of i₃₂ via a loose exit transition state of just 5 kJ mol⁻¹ above the separated products. Intermediates i₃₄ and i₃₅ are connected with i₃₃ via low-lying barriers 15 and 20 kJ mol⁻¹ above i₃₃, respectively. The intermediate i₃₆ can also be formed via isomerization of i₃₅ via a low-lying transition state of 15 kJ mol⁻¹ above i₃₅. The 3-penten-1-yne (p₁₅) product may be formed via atomic hydrogen emission from the CH moiety of i₃₄ and i₃₆ via tight exit transition states lying 22 and 23 kJ mol⁻¹ above the separated products, respectively. The 1,3-hydrogen migration in i₃₆ leads to i₁₁ and a multi-step pathway from i₁₁ described in Section 4.1 and shown in Figure 4 yields the cyclopentadiene (p₁) product. A three-member ring closure in i₃₆ leads to i₃₇, which is connected with i₃₈ via a low-lying rotational transition state 17 kJ mol⁻¹ above i₃₇. The intermediate i₃₈ can also be formed from i₁₇ by atomic hydrogen migration via a transition state lying 206 kJ mol⁻¹ above i₁₇. The 3-ethylidene-cyclopropene (p₁₆) product may be formed via atomic hydrogen emission from CH group of i₃₇ via a tight exit transition state lying 21 kJ mol⁻¹ above the separated products. The cis-3-vinyl-cyclopropene (p₆) and trans-3-vinyl-cyclopropene (p₁₁) products can be accessed via hydrogen emission from the CH₃ group of i₃₈ and i₃₇ with exit transition states lying 33 and 11 kJ mol⁻¹ above the separated products, respectively. In brief, p₁, p₂, p₆, p₁₁, p₁₅, and p₁₆ can be accessed via pathways (27)–(35). Considering the experimentally derived reaction energy of -119 ± 42 kJ mol⁻¹, cis-3-vinyl-cyclopropene (p₆), trans-3-vinyl-cyclopropene (p₁₁) and 3-ethylidene-cyclopropene (p₁₆) with reaction energies of -130 , -135 and -119 are the most likely products. For the cis-3-vinyl-cyclopropene (p₆), the hydrogen loss via pathway (29) requires emission from the CH₂ group of 1,3-butadiene; however, pathways (30) would necessitate the atomic hydrogen emission either from the CH or CH₂ moieties of the 1,3-butadiene reactant. Channel (31) leads to 3-vinyl-cyclopropene (p₁₁) with atomic hydrogen loss, which may originate both from the CH and CH₂ moieties of the 1,3-butadiene reactant. For the 3-ethylidene-cyclopropene (p₁₆) product, hydrogen atom loss proceeds via pathway (34) solely from the CH₂ group of 1,3-butadiene; however, pathway (35) would require the atomic hydrogen to be emitted from the CH moiety of 1,3-butadiene. Therefore, accounting for the results from the isotopic substitution experiments, we can conclude that pathways (29) and (34) leading to formation of

p₆ and p₁₆ may be available under our experimental conditions.



In summary, considering the experimentally derived reaction energy of -119 ± 42 kJ mol⁻¹ and isotopic substitution experiments, cis-3-vinyl-cyclopropene (p₆), trans-3-vinyl-cyclopropene (p₁₁) and 3-ethylidene-cyclopropene (p₁₆) along with atomic hydrogen are likely formed under our experimental conditions. Cis-3-vinyl-cyclopropene (p₆) can be accessed via pathways (8) and (29), while trans-3-vinyl-cyclopropene (p₁₁) and 3-ethylidene-cyclopropene (p₁₆) may be formed via pathways (19) and (34), respectively. Due to high barriers of 219, 215, and 226 kJ mol⁻¹, respectively, isomerization from i₃ to i₇, i₄ to i₂, and i₁₆ to i₁₅ is much less competitive than the conformational changes i₂→i₇, i₃→i₄, and i₄→i₃. Therefore, intermediates i₁₅, i₃₁, i₃₃, and i₃₅–i₃₈ along with pathway (34) likely pay only minor contributions. Consequently, 3-ethylidene-cyclopropene (p₁₆) may not be formed. The most likely products cis-3-vinyl-cyclopropene (p₆) and trans-3-vinyl-cyclopropene (p₁₁) on this reduced PES (Figure 8) can be accessed via pathways (8), (29) and (36) with exit transition

states lying 5, 33 and 7 kJ mol⁻¹ above the separated products, respectively.

Note that **p6** and **p11** are formed via the barrierless addition of the methylidyne radical to the terminal carbon atom and/or the C–C double bond of 1,3-butadiene, but not through insertion of methylidyne into C–H or C–C single bond of 1,3-butadiene under our experimental conditions. Considering the reaction of the methylidyne (CH) radical with ethylene (C₂H₄), Mebel et al.^[46] and Kaiser et al.^[47] proposed a ratio in the entrance channels of carbon–carbon double bond addition and carbon–hydrogen bond insertion of about 85:15, which can be understood in terms of a reduced cone of acceptance of the C–H σ -bond compared to the π electrons of the C–C double bond. The similar reaction dynamics mechanisms of these two systems, methylidyne–1,3-butadiene and methylidyne–ethylene, suggested that methylidyne radical addition to the terminal carbon atom and/or carbon–carbon double bond of 1,3-butadiene is likely the dominant entrance channel, which is consistent with our aforementioned conclusions.

We also explored the statistical yields of products **p1**–**p16** using RRKM theory (Table 2). Since the initial adducts **i1**, **i2**, and **i7** can easily rearrange to **i3** and **i4** via barriers that are lower than dissociation barriers, the resulting product branching ratios from RRKM calculations appear to be practically independent of the initial intermediate. RRKM theory predicts cyclopentadiene (**p1**) along with atomic hydrogen to be the most likely product (~76%) followed by (Z)-3-penten-1-yne (**p9**) (~15%), while trans- and cis-1,2,4-pentatrienes (**p2** and **p3**) are predicted as minor statistical products (~4% each). The formation of cyclopentadiene is statistically preferable due to the low barriers along pathway (2) leads eventually leading to **p1** from **i3** and **i4**. Obviously, the experimental findings observed under single-collision conditions contradict these predictions. These findings can be reconciled by proposing a critical non-RRKM behavior of this bimolecular reaction system leading to cis- (**p6**) and trans-3-vinyl-cyclopropene (**p11**) with a life time of the initial adducts insufficient to allow a complete energy randomization to occur. This behavior was also detected in the related reactions of methylidyne with methylacetylene/allene and propylene.^[24,26] Here, the barrierless cycloaddition of the methylidyne radical to the carbon–carbon triple/double and double bond of methylacetylene/allene and propylene leads eventually leading to triafulvene with atomic hydrogen elimination from the methyl moiety of the methylacetylene reactant and from the CH₂ group of allene; likewise, 1-methylcyclopropene and 3-methylcyclopropene along with atomic hydrogen emission from the vinyl moiety are formed in the methylidyne–propylene system. For the methylidyne–methylacetylene/allene systems,^[24] the initial cycloaddition intermediates were located at –334, –322, and –383 kJ mol⁻¹ below the energies of the separated reactants, respectively. The sole product triafulvene ($\Delta_f G = -171$ kJ mol⁻¹) was formed by atomic hydrogen emission from the initial intermediates via a loose exit transition state lying 6–12 kJ mol⁻¹ above the separated products. Similar reaction dynamics also dominate the methylidyne–propylene system.^[26] The final products 1-methylcyclopropene ($\Delta_f G = -157$ kJ mol⁻¹) and 3-meth-

ylcyclopropene ($\Delta_f G = -143$ kJ mol⁻¹) were formed in the bimolecular reaction of methylidyne and propylene with hydrogen atom loss from the initial intermediates via loose exit transition states located 9–15 kJ mol⁻¹ above the separated products. These initial cycloaddition intermediates were located at –345 and –346 kJ mol⁻¹ below the separated reactants, respectively. Ring-opening and hydrogen migrations are important isomerization processes between intermediates in these reactions, which can eventually lead to several more stable products. However, all experimental findings suggest that the atomic hydrogen emission from the initial cycloaddition intermediates to the final products occurs on a time scale that is faster than any further isomerization. In the gas phase, extensive non-statistical dynamics have been revealed, both experimentally and computationally, which includes PES bifurcations; non-RRKM unimolecular decomposition; non-intrinsic reaction coordinate dynamics; and also roaming dynamics.^[48–57]

5. Conclusion

To conclude, the crossed molecular beam reactions of the methylidyne radical (CH; X²Π) with 1,3-butadiene (CH₂CHCHCH₂; X¹A_g) along with (partially) substituted reactants were conducted at collision energies of 20.8 kJ mol⁻¹. Combining our experimental data with ab initio electronic structure and statistical rate theory calculations, the methylidyne radical is revealed to add barrierlessly to the terminal carbon atom and/or carbon–carbon double bond of 1,3-butadiene, resulting in C₅H₇ intermediates with a lifetime longer than its rotation period. These adducts undergo nonstatistical, unimolecular decomposition via atomic hydrogen loss from the terminal CH₂ moiety of the 1,3-butadiene reactant forming the cyclic cis- (**p6**) and trans-3-vinyl-cyclopropene (**p11**) with overall reaction exoergicities of -119 ± 42 kJ mol⁻¹. These cyclic C₅H₆ isomers can be produced even in low-temperature environments such as cold molecular clouds like TMC-1, since the reaction is barrierless and exoergic, all transition states are below the energy of the separated reactants. Besides, in high-density environments such as combustion flames and circumstellar envelopes of carbon stars, these cyclic C₅H₆ isomers might undergo hydrogen-assisted isomerization to the thermodynamically most stable cyclopentadiene (c-C₅H₆) isomer followed by hydrogen abstraction/loss to the cyclopentadienyl radical (c-C₅H₅), which is considered as a crucial precursor to PAHs and soot.^[58–67] Also, in high-density environments where the energy exchange between internal degrees of freedom can be facilitated by collisions with a bath gas, the behavior of the CH + 1,3-butadiene reaction may be statistical and the reaction itself would be expected to produce cyclopentadiene as a major product.

Supporting Information

See supplementary material for the PES figures with H atoms from methylidyne radical, CH moiety and CH₂ moiety of 1,3-

butadiene reactant highlighted in grey, green and blue, respectively; and optimized Cartesian coordinates (in Å) and calculated vibrational frequencies (in cm⁻¹) of the reactants, products, intermediates, and transition states in the methylidyne radical plus 1,3-butadiene reaction; rate constants for all unimolecular reactions in the CH + 1,3-butadiene system calculated using RRKM theory at $E_{\text{col}} = 20.8 \text{ kJ mol}^{-1}$.

Acknowledgements

This work was supported by the U.S. Department of Energy, Basic Energy Sciences DE-FG02-03ER15411 and DE-FG02-04ER15570 to the University of Hawaii and to Florida International University, respectively. Ab initio calculations at Samara University were supported by the Ministry of Science and Higher Education of the Russian Federation under Grant No. 14.Y26.31.0020.

Conflict of Interest

The authors declare no conflict of interest.

Keywords: gas-phase chemistry • reaction dynamics • reaction intermediates • single-collision conditions • 3-vinylcyclopropene

- [1] N. Hansen, S. J. Klippenstein, J. A. Miller, J. Wang, T. A. Cool, M. E. Law, P. R. Westmoreland, T. Kasper, K. Kohse-Höinghaus, *J. Phys. Chem. A* **2006**, *110*, 4376–4388.
- [2] N. Hansen, J. A. Miller, C. A. Taatjes, J. Wang, T. A. Cool, M. E. Law, P. R. Westmoreland, *Proc. Combust. Inst.* **2007**, *31*, 1157–1164.
- [3] B. Yang, C. Huang, L. Wei, J. Wang, L. Sheng, Y. Zhang, F. Qi, W. Zheng, W.-K. Li, *Chem. Phys. Lett.* **2006**, *423*, 321–326.
- [4] J. Cernicharo, C. Kahane, J. Gomez-Gonzalez, M. Guélin, *Astron. Astrophys.* **1986**, *167*, L5–L7.
- [5] J. Cernicharo, C. Kahane, J. Gomez-Gonzalez, M. Guélin, *Astron. Astrophys.* **1986**, *164*, L1–L4.
- [6] J. Cernicharo, M. Guélin, C. M. Walmsley, *Astron. Astrophys.* **1987**, *172*, L5.
- [7] P. F. Bernath, K. H. Hinkle, J. J. Keady, *Science* **1989**, *244*, 562–564.
- [8] I. Hahndorf, H. Y. Lee, A. M. Mebel, S. H. Lin, Y. T. Lee, R. I. Kaiser, *J. Chem. Phys.* **2000**, *113*, 9622–9636.
- [9] L. C. L. Huang, H. Y. Lee, A. M. Mebel, S. H. Lin, Y. T. Lee, R. I. Kaiser, *J. Chem. Phys.* **2000**, *113*, 9637–9648.
- [10] N. Balucani, H. Y. Lee, A. M. Mebel, Y. T. Lee, R. I. Kaiser, *J. Chem. Phys.* **2001**, *115*, 5107–5116.
- [11] Y. Guo, X. Gu, N. Balucani, R. I. Kaiser, *J. Phys. Chem. A* **2006**, *110*, 6245–6249.
- [12] Y. Guo, X. Gu, F. Zhang, A. M. Mebel, R. I. Kaiser, *J. Phys. Chem. A* **2006**, *110*, 10699–10707.
- [13] A. M. Mebel, V. V. Kislov, R. I. Kaiser, *J. Phys. Chem. A* **2006**, *110*, 2421–2433.
- [14] X. Gu, Y. Guo, F. Zhang, A. M. Mebel, R. I. Kaiser, *Chem. Phys. Lett.* **2007**, *444*, 220–225.
- [15] D. S. N. Parker, F. Zhang, Y. S. Kim, R. I. Kaiser, A. M. Mebel, *J. Phys. Chem. A* **2011**, *115*, 593–601.
- [16] B. B. Dangi, S. Maity, R. I. Kaiser, A. M. Mebel, *J. Phys. Chem. A* **2013**, *117*, 11783–11793.
- [17] C.-M. Gong, H.-B. Ning, Z.-R. Li, X.-Y. Li, *Theor. Chem. Acc.* **2015**, *134*, 1599.
- [18] G. da Silva, *J. Phys. Chem. A* **2017**, *121*, 2086–2095.
- [19] A. M. Thomas, M. Lucas, L. Zhao, J. Liddiard, R. I. Kaiser, A. M. Mebel, *Phys. Chem. Chem. Phys.* **2018**, *20*, 10906–10925.
- [20] A. M. Thomas, L. Zhao, C. He, A. M. Mebel, R. I. Kaiser, *J. Phys. Chem. A* **2018**, *122*, 6663–6672.
- [21] C. He, L. Zhao, A. M. Thomas, G. R. Galimova, A. M. Mebel, R. I. Kaiser, *Phys. Chem. Chem. Phys.* **2019**, *21*, 22308–22319.
- [22] F. Zhang, Y. S. Kim, L. Zhou, A. H. H. Chang, R. I. Kaiser, *J. Chem. Phys.* **2008**, *129*, 134313.
- [23] R. I. Kaiser, P. Maksyutenko, C. Ennis, F. Zhang, X. Gu, S. P. Krishtal, A. M. Mebel, O. Kostko, M. Ahmed, *Faraday Discuss.* **2010**, *147*, 429–478.
- [24] A. M. Thomas, L. Zhao, C. He, G. R. Galimova, A. M. Mebel, R. I. Kaiser, *Angew. Chem. Int. Ed.* **2019**, *58*, 15488–15495.
- [25] C. He, A. M. Thomas, G. R. Galimova, A. N. Morozov, A. M. Mebel, R. I. Kaiser, *J. Am. Chem. Soc.* **2020**, *142*, 3205–3213.
- [26] C. He, A. M. Thomas, G. R. Galimova, A. M. Mebel, R. I. Kaiser, *J. Phys. Chem. A* **2019**, *123*, 10543–10555.
- [27] G. O. Brink, *Rev. Sci. Instrum.* **1966**, *37*, 857–860.
- [28] N. R. Daly, *Rev. Sci. Instrum.* **1960**, *31*, 264–267.
- [29] P. S. Weiss, Ph. D. Dissertation Thesis, University of California: Berkeley, CA, **1986**.
- [30] M. F. Vernon, Ph. D. Dissertation thesis, University of California: Berkeley, CA, **1983**.
- [31] A. D. Becke, *J. Chem. Phys.* **1993**, *98*, 5648–5652.
- [32] C. Lee, W. Yang, R. G. Parr, *Phys. Rev. B* **1988**, *37*, 785–789.
- [33] T. B. Adler, G. Knizia, H.-J. Werner, *J. Chem. Phys.* **2007**, *127*, 221106.
- [34] G. Knizia, T. B. Adler, H.-J. Werner, *J. Chem. Phys.* **2009**, *130*, 054104.
- [35] T. H. Dunning Jr., *J. Chem. Phys.* **1989**, *90*, 1007–1023.
- [36] H.-J. Werner, P. J. Knowles, R. Lindh, F. R. Manby, M. Schütz, P. Celani, T. Korona, G. Rauhut, R. D. Amos, A. Bernhardsson, MOLPRO, Version 2010.1, A Package of Ab Initio Programs., University of Cardiff: Cardiff: UK, **2010**.
- [37] J. Zhang, E. F. Valeev, *J. Chem. Theory Comput.* **2012**, *8*, 3175–3186.
- [38] Gaussian 09 (Revision A.1), M. J. Frisch, G. W. Trucks, H. B. Schlegel, G. E. Scuseria, M. A. Robb, J. R. Cheeseman, G. Scalmani, V. Barone, B. Mennucci, G. A. Petersson, H. Nakatsuji, M. Caricato, X. Li, H. P. Hratchian, A. F. Izmaylov, J. Bloino, G. Zheng, J. L. Sonnenberg, M. Hada, M. Ehara, K. Toyota, R. Fukuda, J. Hasegawa, M. Ishida, T. Nakajima, Y. Honda, O. Kitao, H. Nakai, T. Vreven, J. A. Montgomery, Jr., J. E. Peralta, F. Ogliaro, M. Bearpark, J. J. Heyd, E. Brothers, K. N. Kudin, V. N. Staroverov, R. Kobayashi, J. Normand, K. Raghavachari, A. Rendell, J. C. Burant, S. S. Iyengar, J. Tomasi, M. Cossi, N. Rega, J. M. Millam, M. Klene, J. E. Knox, J. B. Cross, V. Bakken, C. Adamo, J. Jaramillo, R. Gomperts, R. E. Stratmann, O. Yazyev, A. J. Austin, R. Cammi, C. Pomelli, J. W. Ochterski, R. L. Martin, K. Morokuma, V. G. Zakrzewski, G. A. Voth, P. Salvador, J. J. Dannenberg, S. Dapprich, A. D. Daniels, Ö. Farkas, J. B. Foresman, J. V. Ortiz, J. Cioslowski, and D. J. Fox, Gaussian, Inc., Wallingford CT, **2009**, 200, 28.
- [39] J. I. Steinfeld, J. S. Francisco, W. L. Hase, *Chemical Kinetics and Dynamics*, Prentice Hall Englewood Cliffs (New Jersey), **1982**.
- [40] H. Eyring, S. H. Lin, S. M. Lin, *Basic Chemical Kinetics*, John Wiley and Sons, Inc., New York, **1980**.
- [41] P. J. Robinson, K. A. Holbrook, *Unimolecular Reactions*, Wiley: New York, **1972**.
- [42] C. He, L. Zhao, A. M. Thomas, A. N. Morozov, A. M. Mebel, R. I. Kaiser, *J. Phys. Chem. A* **2019**, *123*, 5446–5462.
- [43] V. V. Kislov, T. L. Nguyen, A. M. Mebel, S. H. Lin, S. C. Smith, *J. Chem. Phys.* **2004**, *120*, 7008–7017.
- [44] D. R. Herschbach, *Discuss. Faraday Soc.* **1962**, *33*, 149–161.
- [45] R. D. Levine, *Molecular Reaction Dynamics*, Cambridge University Press, Cambridge, **2005**.
- [46] J. M. Ribeiro, A. M. Mebel, *J. Phys. Chem. A* **2016**, *120*, 1800–1812.
- [47] F. Zhang, P. Maksyutenko, R. I. Kaiser, *Phys. Chem. Chem. Phys.* **2012**, *14*, 529–537.
- [48] X. Ma, W. L. Hase, *Philos. Trans. R. Soc. A* **2017**, *375*, 20160204.
- [49] P. Manikandan, J. Zhang, W. L. Hase, *J. Phys. Chem. A* **2012**, *116*, 3061–3080.
- [50] L. Sun, W. L. Hase, *J. Chem. Phys.* **2004**, *121*, 8831–8845.
- [51] H. Wang, E. M. Goldfield, W. L. Hase, *J. Chem. Soc. Faraday Trans.* **1997**, *93*, 737–746.
- [52] J. G. López, G. Vayner, U. Lourderaj, S. V. Addepalli, S. Kato, W. A. deJong, T. L. Windus, W. L. Hase, *J. Am. Chem. Soc.* **2007**, *129*, 9976–9985.
- [53] J. Xie, W. L. Hase, R. Otto, R. Wester, *J. Chem. Phys.* **2015**, *142*, 244308.
- [54] A. A. Viggiano, R. A. Morris, J. S. Paschkewitz, J. F. Paulson, *J. Am. Chem. Soc.* **1992**, *114*, 10477–10482.
- [55] R. Spezia, J.-Y. Salpin, M.-P. Gaigeot, W. L. Hase, K. Song, *J. Phys. Chem. A* **2009**, *113*, 13853–13862.
- [56] S. C. Ammal, H. Yamataka, M. Aida, M. Dupuis, *Science* **2003**, *299*, 1555–1557.

- [57] D. Townsend, S. A. Lahankar, S. K. Lee, S. D. Chambreau, A. G. Suits, X. Zhang, J. Rheinecker, L. B. Harding, J. M. Bowman, *Science* **2004**, *306*, 1158–1161.
- [58] N. Hansen, W. Li, M. E. Law, T. Kasper, P. R. Westmoreland, B. Yang, T. A. Cool, A. Lucassen, *Phys. Chem. Chem. Phys.* **2010**, *12*, 12112–12122.
- [59] M. Baroncelli, Q. Mao, S. Galle, N. Hansen, H. Pitsch, *Phys. Chem. Chem. Phys.* **2020**, DOI: 10.1039/c1039cp05854k.
- [60] N. Hansen, T. Kasper, S. J. Klippenstein, P. R. Westmoreland, M. E. Law, C. A. Taatjes, K. Kohse-Höinghaus, J. Wang, T. A. Cool, *J. Phys. Chem. A* **2007**, *111*, 4081–4092.
- [61] M. Baroncelli, D. Felsmann, N. Hansen, H. Pitsch, *Combust. Flame* **2019**, *204*, 320–330.
- [62] N. Hansen, J. A. Miller, S. J. Klippenstein, P. R. Westmoreland, K. Kohse-Höinghaus, *Combust. Explos. Shock +* **2012**, *48*, 508–515.
- [63] J. A. Miller, M. J. Pilling, J. Troe, *Proc. Combust. Inst.* **2005**, *30*, 43–88.
- [64] M. Frenklach, A. Mebel, *Phys. Chem. Chem. Phys.* **2020**, *22*, 5314–5331.
- [65] M. Frenklach, *Phys. Chem. Chem. Phys.* **2002**, *4*, 2028–2037.
- [66] R. I. Singh, A. M. Mebel, M. Frenklach, *J. Phys. Chem. A* **2015**, *119*, 7528–7547.
- [67] X. You, D. Y. Zubarev, W. A. Lester Jr, M. Frenklach, *J. Phys. Chem. A* **2011**, *115*, 14184–14190.

Manuscript received: March 5, 2020

Revised manuscript received: April 12, 2020

Accepted manuscript online: April 14, 2020

Version of record online: May 25, 2020
